Supporting Information

First examples of room-temperature discotic nematic liquid crystals exhibiting ambipolar charge carrier mobilities

*Monika Gupta**, [a], Abhinand Krishna KM, [a] Simran Sony, [a] Shallu Dhingra, [b] Asmita Shah, [c] and Dharmendra Pratap Singh, [c]*

[a] Department of Chemistry, Indian Institute of Technology Ropar (IIT-Ropar) Bara Phool, Punjab-140001, India.

[b] Department of Chemical Sciences, Indian Institute of Science Education and Research (IISER) Mohali, Sector-81, Sahibzada Ajit Singh Nagar, Knowledge City, Manauli 140306, India.

[c] Université du Littoral Côte d'Opale, UR 4476, UDSMM, Unité de Dynamique et Structure des Matériaux Moléculaires, F-62228 Calais, France.

*Corresponding author: Tel.: +91-1881-232074; E-mail: monika.gupta@iitrpr.ac.in

Table of Contents

1. Experimental Section

1.1. Materials and Reagents

Chemicals and solvents were all of AR quality and were used without further purification. Chemicals were purchased from Sigma–Aldrich (Bangalore, India), TCI and Avra Synthesis Pvt. Ltd. Column chromatographic separations were performed on silica gel (60-120, 100-200 & 230-400 mesh). Thin layer chromatography (TLC) was performed on aluminium sheets pre-coated with silica gel (Merck, Kieselgel 60, F254).

1.2. Synthesis and characterization of target compounds (1 - 4)

Compounds **6**, **7** and corresponding alkyl bromides **8-11** were prepared as according to the previous reports.[1-5]

For the synthesis of compound **1**, compound **7** (1 equivalent) was dissolved in water (15 ml) followed by the addition of Potassium hydroxide (KOH, 1.1 equivalents), compound **8** (1.5 equivalents) and Tetraoctylammonium bromide (TOAB, 0.09 equivalents). The contents were refluxed for five hours. The reaction mixture was cooled to room-temperature and the organic contents were extracted with dichloromethane (DCM). The organic layer was dried over anhydrous sodium sulphate and concentrated. The resulting residue was then purified through column chromatography over silica gel using hexane and DCM. The pure compound was eluted at 45% DCM in hexane. The dried compound was further re-precipitated by first dissolving in a minimum amount of DCM and then adding excess of methanol, to remove any residual impurities and to obtain pure compound **1** (0.219 g, Yield: 70%, Colour: white).

Compounds **2**, **3** and **4** were prepared through similar procedure as reported above. Compound **2** was eluted at 30% DCM in hexane and reprecipitated using DCM and methanol to obtain pure compound **2** (0.271 g, Yield: 70%, Colour: White). Compound **3** and **4** were eluted at 10% and 40% dichloromethane in hexane, respectively and reprecipitated using DCM and methanol to obtain pure compounds **3** (0.165 g, Yield: 58%, Colour: Yellow) and **4** (0.150 g, Yield: 55%, Colour: off-white), respectively.

All the synthesized compounds were characterized by ^{1}H NMR, ^{13}C NMR, IR, UV-Vis and mass spectrometry as shown below:

Compound 6

^{1}H NMR (400 MHz, $CDCl_3$, δ in ppm): 7.25 (s, 2H), 4.0 (m, 6H), 3.88 (s, 3H), 1.76 (m, 6H), 1.47 (p, 6H, J = 4, 8, 8, 8 Hz), 1.26 (m, 36H), 0.87 (t, 9H, J = 8, 4 Hz).

Compound 7

^{1}H NMR (400 MHz, $CDCl_3$, δ in ppm): 7.32 (s, 2H), 4.04 (q, 6H, J = 4, 8 Hz), 1.78 (m, 6H), 1.47 (m, 6H), 1.3 (m, 36H), 0.88 (t, 9H, J = 8 Hz).

Compound 8

^{1}H NMR (400 MHz, $CDCl_3$, δ in ppm): 7.68 (m, 4H), 7.53 (m, 2H), 7.0 (m, 2H), 4.0 (t, 2H, J = 8, 4 Hz), 3.41 (t, 2H, J = 8, 4 Hz), 1.83 (m, 4H), 1.45 (m, 2H), 1.31 (m, 10H).

Compound 9

^{1}H NMR (400 MHz, $CDCl_3$, δ in ppm): 5.36 (s, 1H), 4.62 (d, 1H, J = 8 Hz), 3.40 (m, 2H), 2.28 (m, 4H), 1.98 (t, 2H, J = 12 Hz), 1.84 (m, 4H), 1.28 (m, 42H), 0.92 (d, 2H, J = 8 Hz), 0.85 (m, 6H).

Compound 10

^{1}H NMR (400 MHz, $CDCl_3$, δ in ppm): 7.50 (m, 10H), 7.15 (m, 10H), 4.33 (t, 2H, J = 8 Hz), 3.49 (t, 2H, J = 8, 4 Hz), 2.61 (t, 2H, J = 8 Hz), 1.90 (m, 4H), 1.58 (m, 10H), 1.31 (m, 30H), 0.84 (m, 15H).

Compound 11

^{1}H NMR (400 MHz, $CDCl_3$, δ in ppm): 7.25 (s, 2H), 4.23 (t, 2H, J = 8 Hz), 3.41 (t, 2H, J = 4 Hz), 1.92 (m, 4H), 1.75 (m, 10H), 1.58 (m, 10H), 1.28 (m, 32H), 0.87 (m, 15H).

Compound 1

FT-IR (cm^{-1}): 2919.23, 2849.94, 2223.29, 1706.49, 1654.23, 1601.80, 1588.85, 1560.22, 1494.50, 1466.95, 1430.14, 1383.63, 1335.51, 1290.54, 1218.76, 1180.64, 1118.02, 1028.11, 1009.37, 979.08, 888.51, 821.47, 815.03, 768.02, 721. 45, 661.29, 596.76, 562.61, 531.33.

UV-vis (nm): 295

^{1}H NMR (400 MHz, $CDCl_3$, δ in ppm): 7.70 (q, 4H, J = 8, 12, 8 Hz), 7.52 (d, 2H, J = 8 Hz), 7.25 (s, 2H), 6.99 (d, 2H, J = 12Hz), 4.28 (t, 2H, J = 8, 4 Hz), 4.02 - 3.98 (m, 8H), 1.84 -1.70 (m, 10H), 1.49 - 1.41 (m, 10H), 1.34 - 1.25 (m, 44H), 0.88 (t, 9H, J = 4, 8 Hz).

^{13}C NMR (100 MHz, $CDCl_3$, δ in ppm): 166.52, 159.76, 152.76, 145.26, 142.29, 132.55, 131.23,128.30, 127.05, 125.02, 119.11, 115.04, 110.0, 107.96, 73.49, 69.15, 68.11, 65.11, 31.90, 30.30, 29.71, 29.63, 29.58, 29.46, 29.39, 29.34, 29.29, 29.24, 28.72, 26.07, 26.04, 25.98, 22.68, 14.11.

MS: $[M+H]^+$ Calculated for $C_{60}H_{93}NO_6$ 924.3572; found 924.7080.

Elemental analysis (%): Calculated C 77.96 H 10.14 N 1.52. Found C 77.82 H 10.47 N 1.72.

Compound 2

FT-IR (cm^{-1}): 2914.98, 2848.25, 1733.97, 1713.47, 1589.16, 1499.49, 1464.60, 1434.33, 1387.76, 1332.60, 1245.19, 1215.67, 1110.97, 1065.25, 1029.53, 1013.45, 974.42, 924.87, 881.82, 860.67, 798.40, 777.36, 786.41, 719.83.

UV-vis (nm): 287

^{1}H NMR (400 MHz, $CDCl_3$, δ in ppm): 7.24 (s, 2H), 5.37 (d, 1H, J = 4 Hz), 4.65 - 4.57 (m, 1H), 4.27 (t, 2H, J = 8, 4 Hz), 4.01 (t, 6H, J = 4 Hz), 2.31 - 2.24 (m, 4H), 2.03 - 1.93 (m, 2H), 1.87- 1.75 (m, 12H), 1.56 - 1.43 (m, 12H), 1.34 - 1.19 (m, 58H), 1.15 - 0.98 (m, 12H), 0.90 - 0.84 (m, 18H).

^{13}C NMR (100 MHz, $CDCl_3$, δ in ppm): 173.30, 166.51, 152.76, 142.25, 139.68, 125.03,122.58, 107.93, 73.67, 73.48, 69.13, 65.13, 56.65, 56.09, 49.98, 42.28, 39.70, 39.49, 38.13, 36.97, 36.57, 36.15, 35.78, 34.68, 31.91, 30.30, 29.63, 29.58, 29.46, 29.39, 29.35, 29.29, 29.08, 28.21, 28.00, 27.79, 26.09, 25.99, 23.80, 22.81, 22.68, 22.55, 14.11, 11.83.

MS: $[M+H]^+$ Calculated for $C_{75}H_{130}O_7$ 1143.9894; found 1143.9884.

Elemental analysis (%): Calculated C 78.75 H 11.46. Found C 78.72 H 11.84.

Compound 3

FT-IR (cm^{-1}): 2915.05, 2848.22, 1713.65, 1590.57, 1500.16, 1464.13, 1435.07, 1388.97, 1333.05, 1257.58, 1245.37, 1219.84, 1110.38, 1016.42, 973.94, 924.93, 882.64, 860.90, 798.04, 766.30, 719.09, 622.66, 545.21.

UV-vis (nm): 286, 339, 380, 420

^{1}H NMR (400 MHz, $CDCl_3$, δ in ppm): 7.56 - 7.50 (m, 10H), 7.25 (s, 2H), 7.22 - 7.16 (m, 10H), 4.36 (t, 2H, J = 4, 8 Hz), 4.27 (t, 2H, J = 8 Hz), 4.00 (t, 6H, J = 8, 4 Hz), 2.63 (t, 10H, J = 8 Hz), 1.92 (qui, 2H, J = 8, 8, 8, 4 Hz), 1.84 - 1.70 (m, 10H), 1.68- 1.62 (m, 10H), 1.49-1.42 (m, 10H), 1.35 – 1.26 (m, 62H), 0.93 - 0.83 (m, 24H).

^{13}C NMR (100 MHz, $CDCl_3$, δ in ppm): 166.50, 160.19, 152.76, 144.00, 143.88, 143.69, 131.75, 131.63, 131.57, 128.73, 128.51, 120.51, 120.45,120.07, 107.93, 99.51, 99.33, 97.28, 87.05, 84.06, 74.72, 73.47, 69.13, 65.16, 37.08, 35.95, 31.91, 31.46, 30.58, 30.31, 30.03, 29.69, 29.59, 29.39, 29.36, 29.30, 26.76, 26.36, 26.05, 22.69, 22.53, 14.11, 14.03.

MS: M^+ Calculated for $C_{118}H_{160}O_6$ 1673.2214; found 1673.8955.

Elemental analysis (%): Calculated C 84.64 H 9.63. Found C 84.49 H 9.82.

Compound 4

FT-IR (cm^{-1}): 2919.64, 2857.03, 1711.27, 1616.97, 1588.36, 1517.55, 1466.70, 1431.27, 1368.89, 1335.18, 1260.03, 1221.85, 1172.11, 1117.98, 1068.96, 1049.58, 925.60, 860.61, 836.32, 762.89, 722.58, 615.03, 602.15.

UV-vis (nm): 285, 308, 345

^{1}H NMR (400 MHz, $CDCl_3$, δ in ppm): 7.84 (s, 6H), 7.25 (s, 2H), 4.29 (t, 2H, J = 4, 8 Hz), 4.23 (t, 12H, J = 8, 4 Hz), 4.01 (t, 6H, J = 8, 4 Hz), 1.95 (qui, 12H, J = 8, 4 , 8, 8 Hz), 1.85 - 1.71 (m, 8H), 1.62 - 1.55 (m, 12H), 1.47 - 1.27 (m, 72H), 0.94 (t, 15H, J = 8 Hz), 0.88 (t, 9H, J = 8 Hz).

^{13}C NMR (100 MHz, $CDCl_3$, δ in ppm): 166.50, 152.74, 148.88, 142.22, 125.01, 123.54, 107.91, 107.22, 73.46, 69.62, 69.10, 65.11, 31.89, 30.29, 29.70, 29.64, 29.61, 29.61, 29.56, 29.55, 29.47, 29.38, 29.33, 29.27, 26.19, 26.06, 26.03, 26.00, 25.83, 22.64, 14.04.

MS: $[M+H]^+$ Calculated for $C_{95}H_{156}O_{11}$ 1474.1712; found 1474.1736.

Elemental analysis (%): Calculated C 77.40 H 10.67. Found C 77.12 H 10.63.

1.3. Instrumental

1.3.1. Structural characterization. Structural characterization of the compound was carried out through a combination of infrared spectroscopy (Thermo Fischer Scientific Nicolet iS50

FT-IR spectrometer with ATR assembly having a smart iTX diamond crystal), ^{1}H NMR and ^{13}C NMR (Jeol JNM ECS 400 MHz NMR spectrometer), UV-Vis spectrophotometer (Shimadzu UV-2600 spectrophotometer) and mass spectrometry (Waters Xevo G2-XS QToF). NMR spectra were recorded using deuterated chloroform ($CDCl_3$) as solvent and tetramethylsilane (TMS) as an internal standard. Elemental analysis was carried out on Thermo Fischer Scientific Elemental Analyzer Model Flash 2000 at a Furnace temperature of 950 °C. Carrier (He) gas with flow of 140 mL/min was employed. The acquisition time was kept 600 seconds. The samples under study were packed in tin capsule for analysis.

1.3.2. Thermogravimetric Analysis. Thermogravimetric analysis (TGA) was carried out from 25 to 500 °C (at a heating rate of 10 °C min^{-1}) under nitrogen atmosphere on a TGA/DSC 1 instrument with an SDTA sensor (Mettler-Toledo). The thermal data were analyzed in the STARe software (version 12.1).

1.3.3. Differential Scanning Calorimetry. Phase transition temperatures were recorded using a TA Instruments Q1000 Differential Scanning Calorimeter and DSC1/700 W with an HSS8 sensor instrument (Mettler Toledo) with a Huber TC100MT Intercooler using an aluminum pan with a pin as a reference.

1.3.4. Polarized Optical Microscopy. Textural observations of the mesophase were performed with Zeiss Axio Imager.A1 polarising microscope provided with a Linkam heating stage (TMS 94). All images were captured using a Infinity 2 camera.

1.3.5 X-ray Diffraction. X-ray diffraction (XRD) was carried out on powder samples using Cu Kα (λ=1.54 Å) radiation from a source (GeniX 3D, Xenocs) operating at 50 kV and 0.6 mA. The diffraction patterns were collected on a two module Pilatus detector.

1.3.6. Rheology. An Anton Paar MCR 102 rheometer with a 25 mm parallel-plate configuration was used to investigate the flow properties of compounds.

1.3.7. Time-of-Flight Studies. The ToF technique equipped with a Nd:YAG pulsed laser having an excitation wavelength of 355 nm and 5 ns pulse width was employed. The LC compounds were first filled in LC cells of thickness ≈ 8.9 μm in the isotropic phase and subsequently cooled with a slow cooling rate to obtain the best molecular ordering as the value of mobility remarkably depends upon the molecular ordering.[3] The LC compounds were irradiated by a laser pulse and displacements of holes/electrons have been recorded on a

digital oscilloscope (Keysight, DSOX3022T) under the application of an external positive and negative voltages in the range of ± 20 to ± 30 V (for compound **4**) and ± 220 to ± 300 V (for compound **3**) with the help of Keithley 6487 voltage source. Unfortunately, the transient photocurrent signals for compounds **1** and **2** were not observed. For the temperature-dependent measurements, the temperature was controlled by custom-made EUROTHERM temperature controller with an accuracy of ± 0.01°C. The output transient photocurrent curves were used to calculate the hole and electron mobility by using the formula; $\mu_{(h,e)} = d^2 / V.\tau$ where, τ is the transit time obtained by photocurrent curves, V is the applied voltage and d is the thickness of ITO sample cells.

2. NMR Spectra

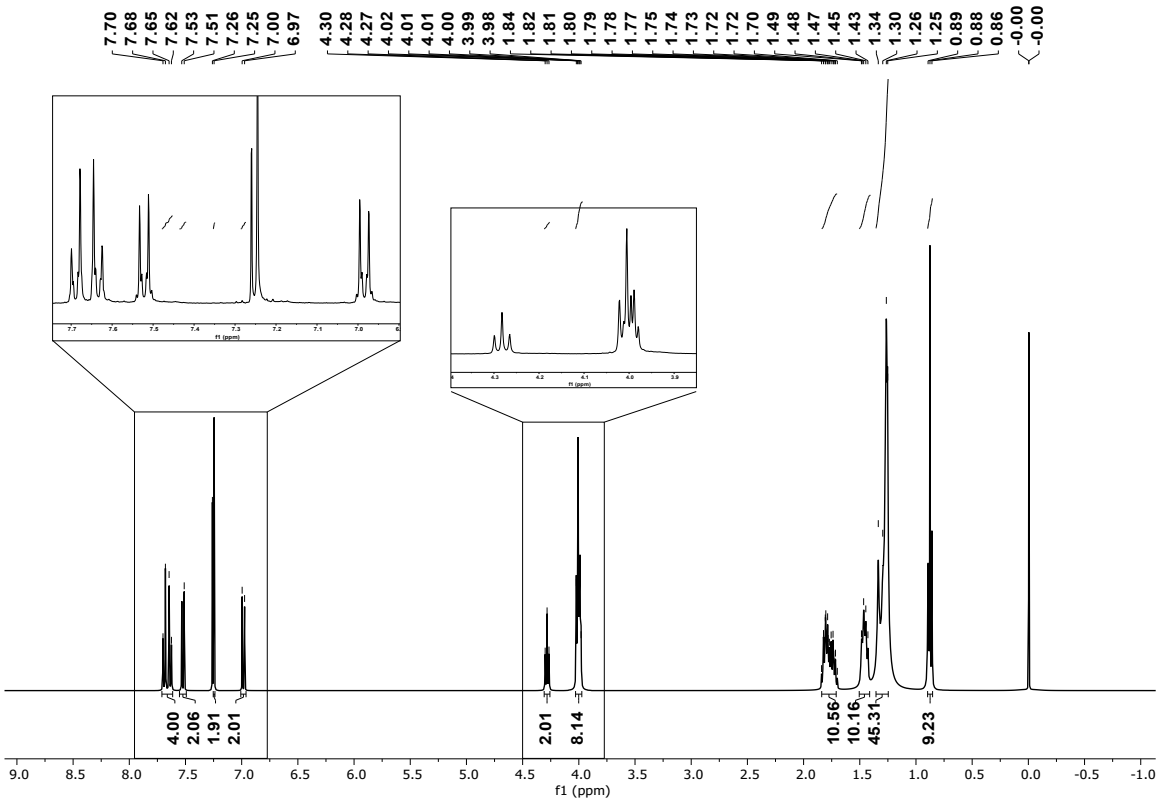

Fig. S1 ^{1}H NMR spectrum of compound **1**.

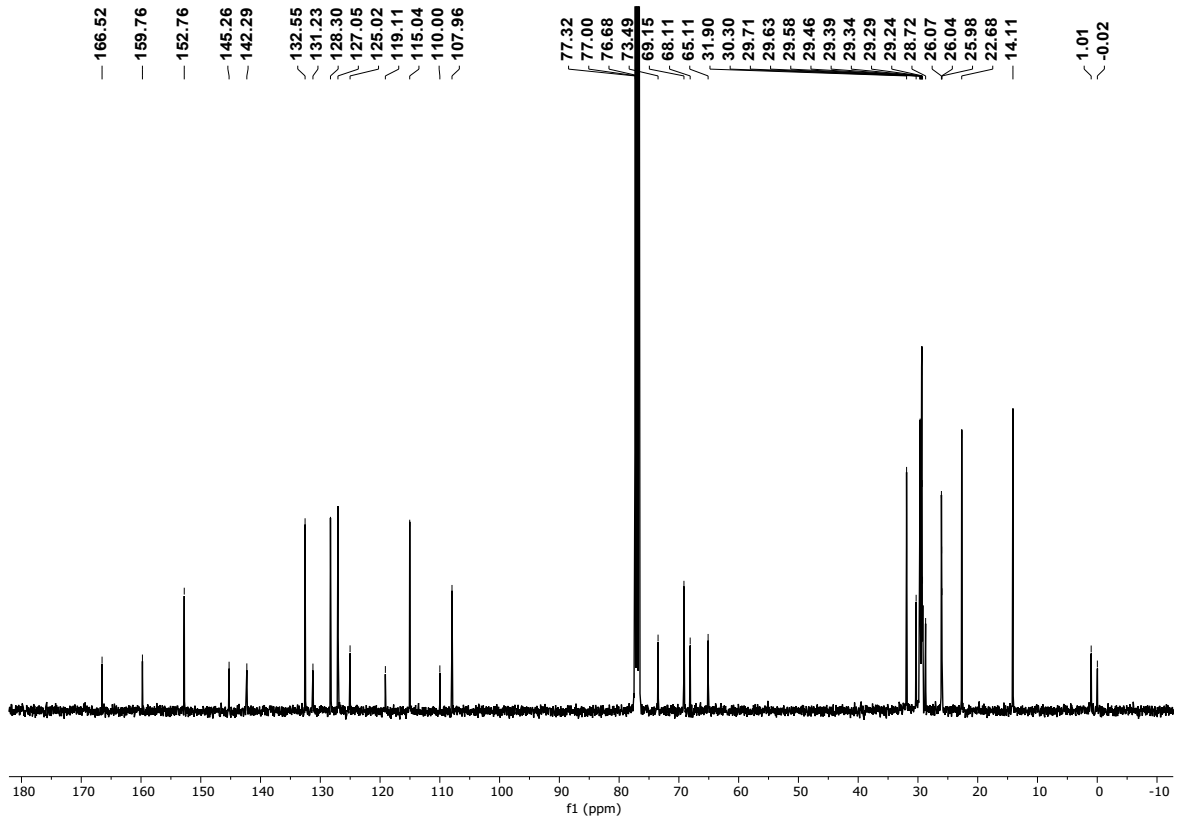

Fig. S2 ^{13}C NMR spectrum of compound **1**.

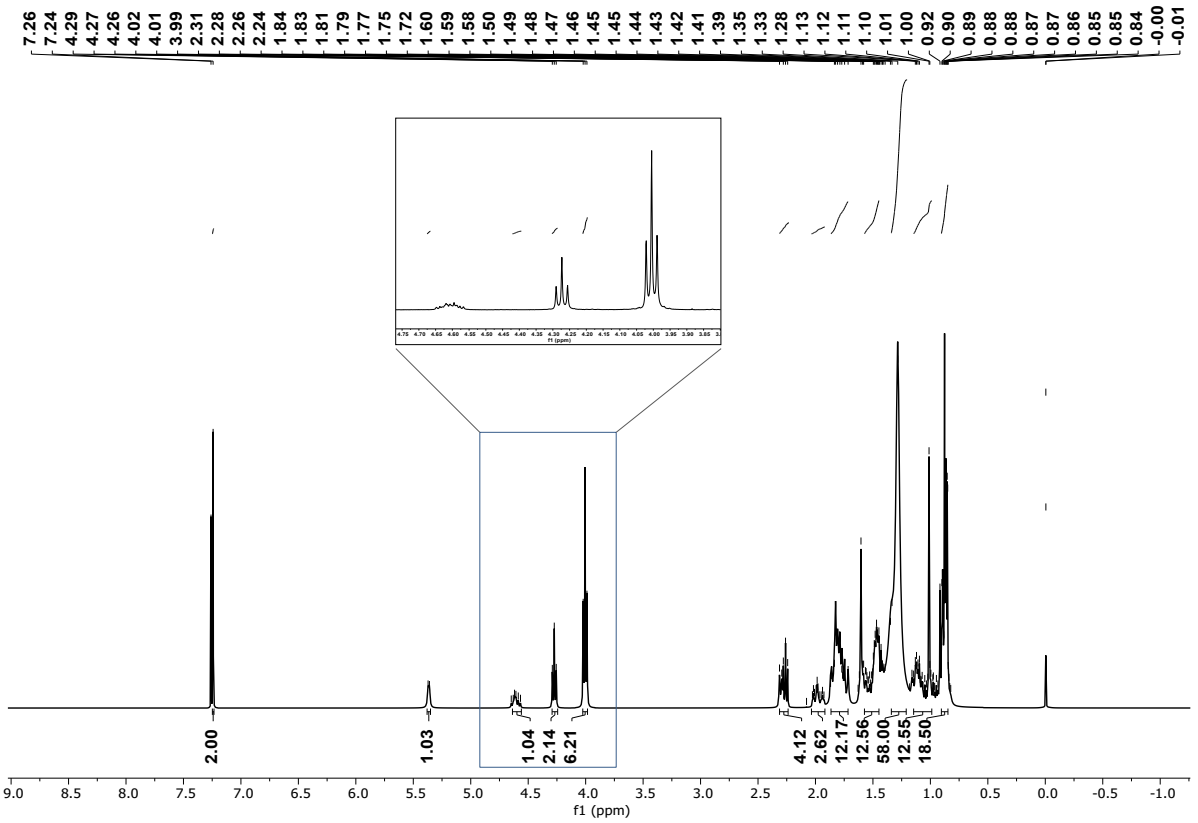

Fig. S3 ^{1}H NMR spectrum of compound **2**.

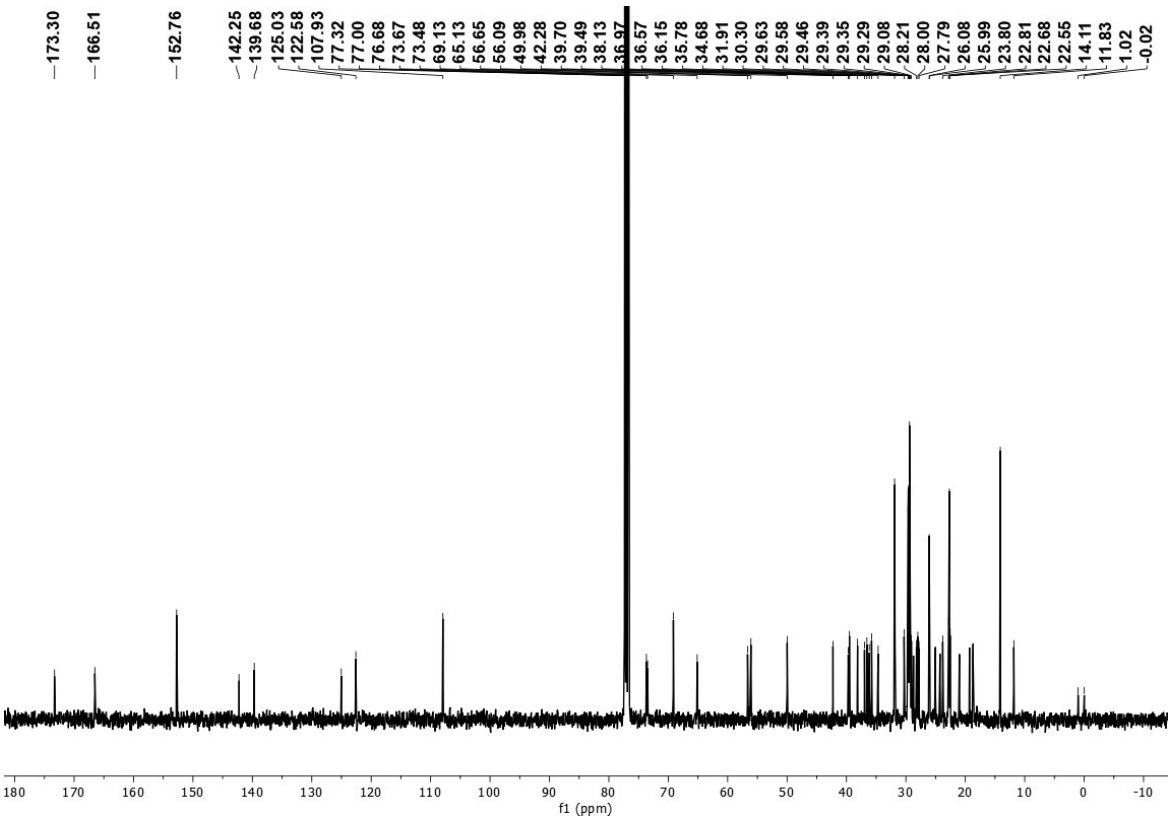

Fig. S4 ^{13}C NMR spectrum of compound **2**.

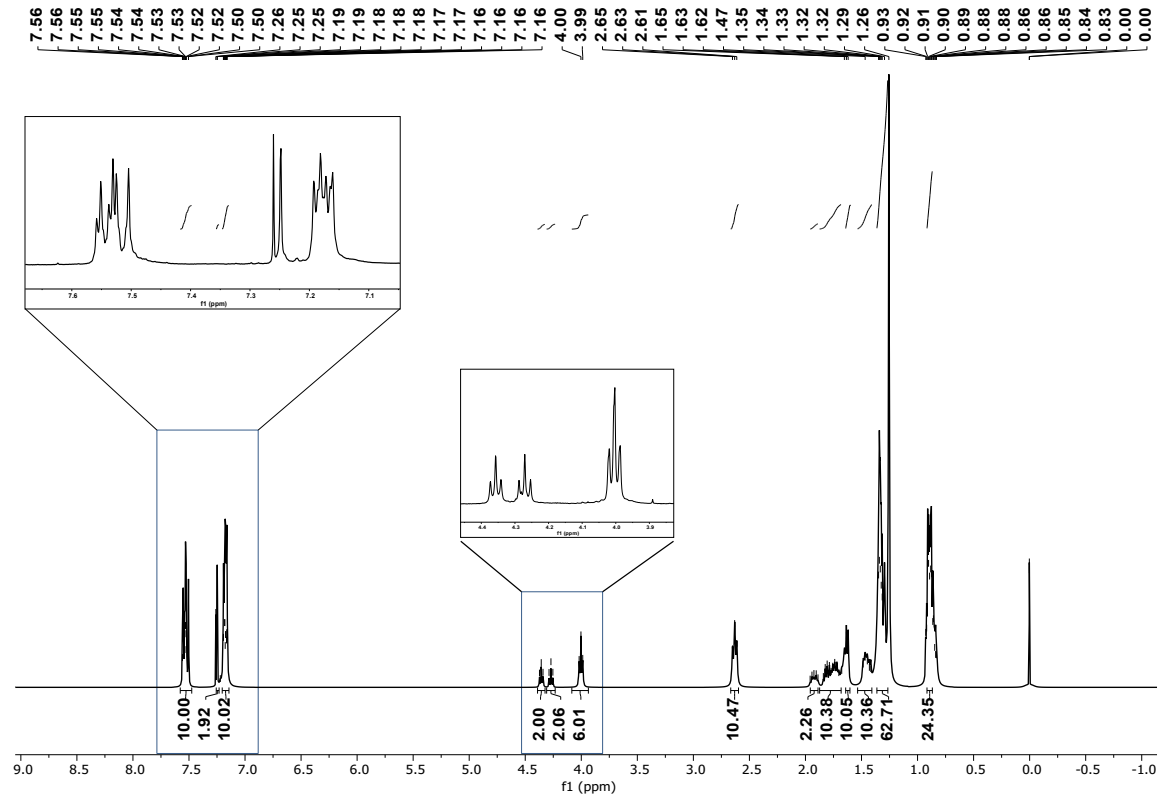

Fig. S5 ^{1}H NMR spectrum of compound **3**.

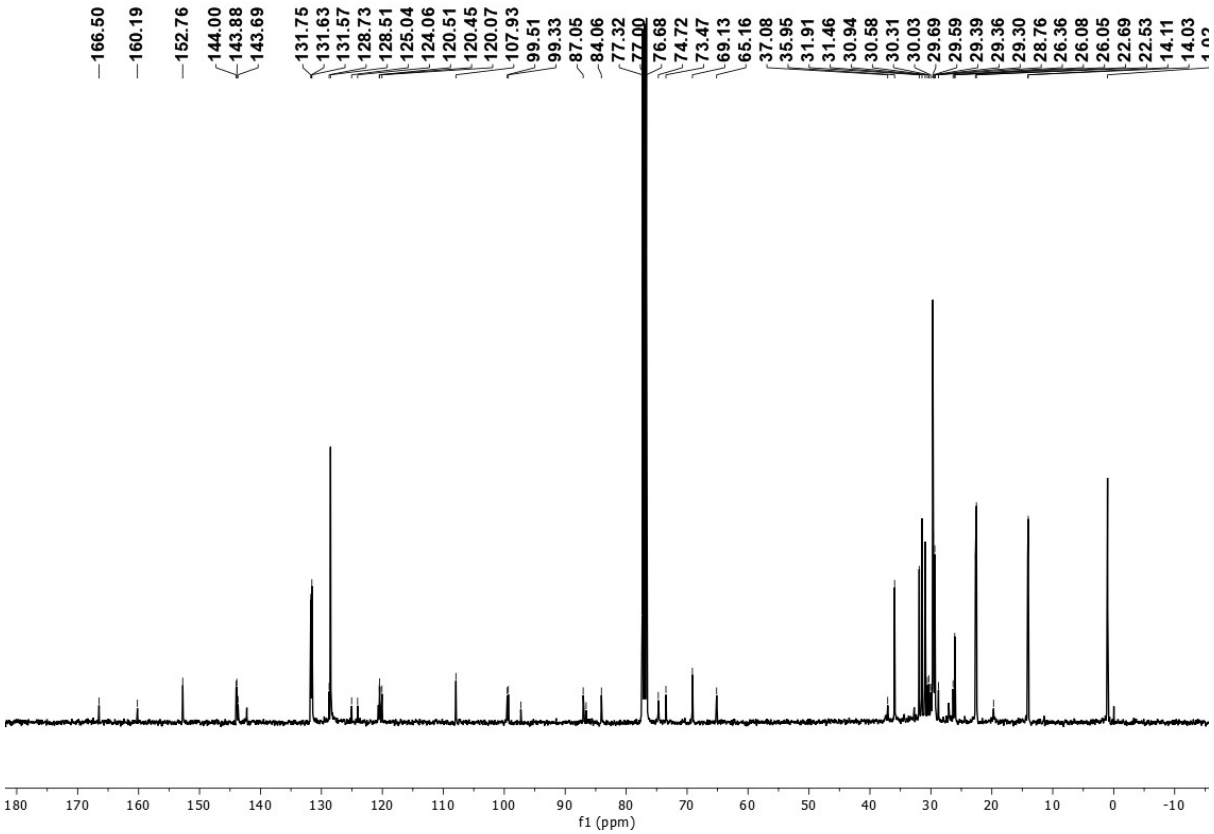

Fig. S6 ^{13}C NMR spectrum of compound **3**.

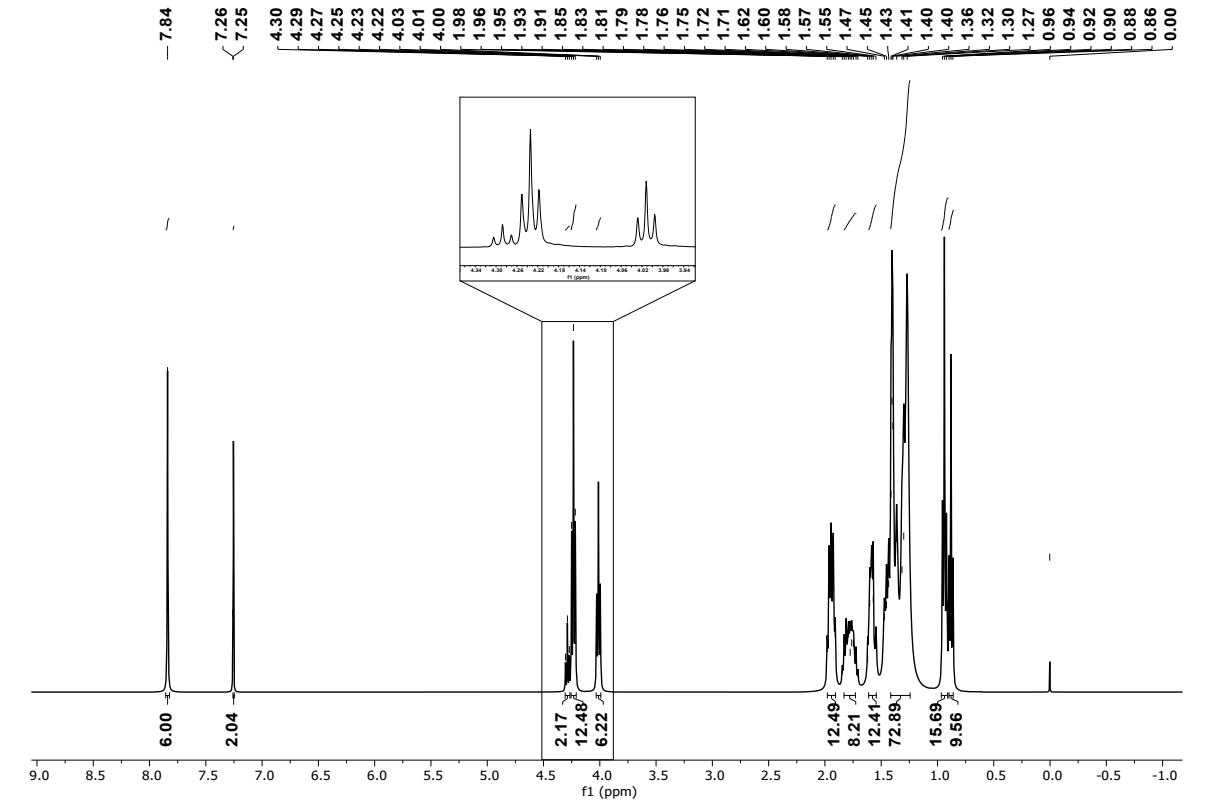

Fig. S7 ^{1}H NMR spectrum of compound **4**.

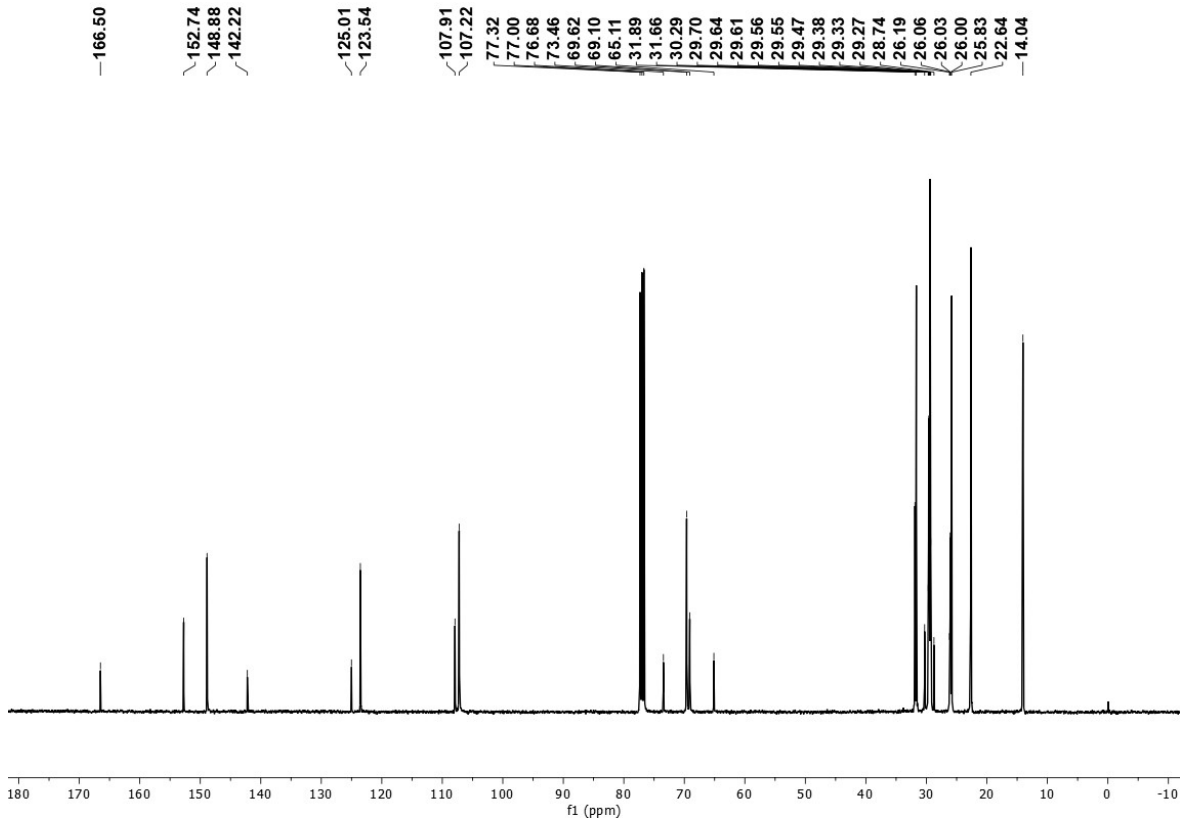

Fig. S8 ^{13}C NMR spectrum of compound **4**.

3. Photophysical studies

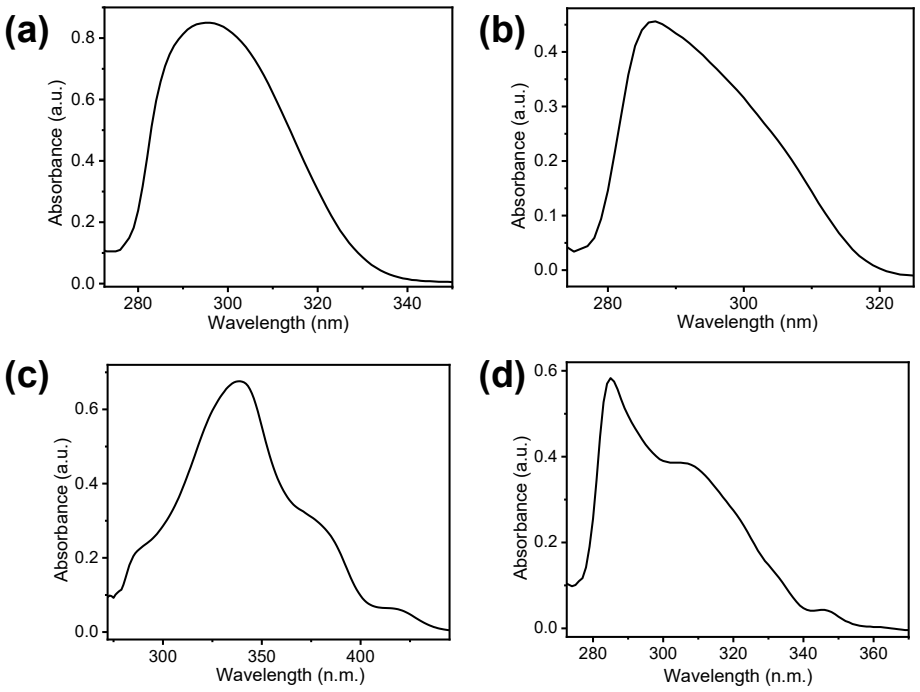

Fig. S9 UV-vis absorption spectra of compound (a) **1**, (b) **2**, (c) **3** and (d) **4** in solution (5 μM in dichloromethane).

4. TGA Curves

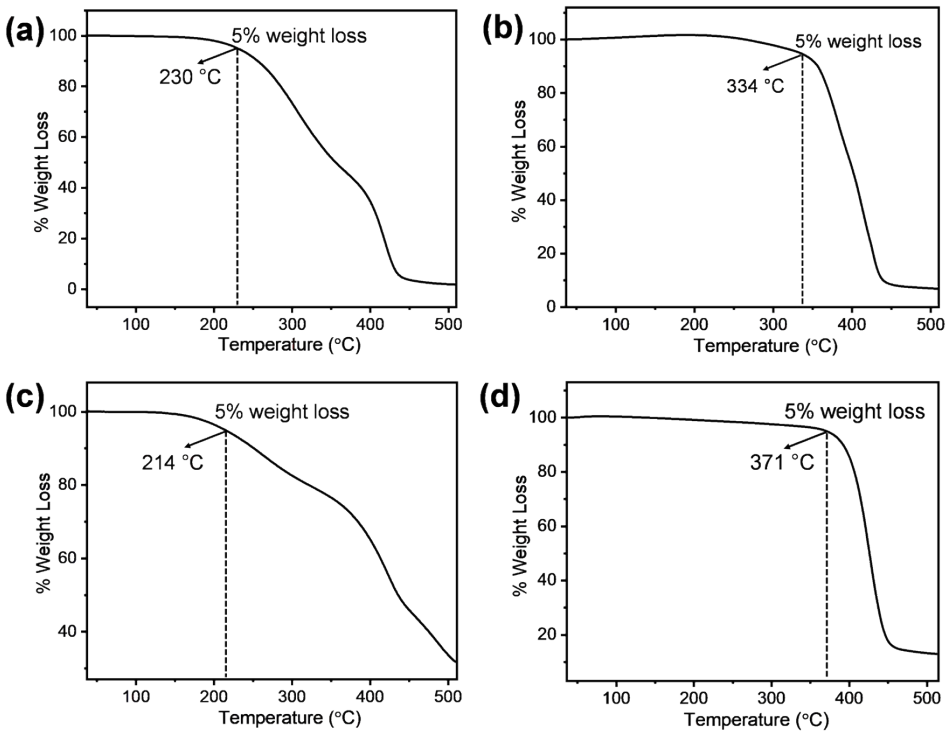

Fig. S10 TGA curves of compound (a) **1**, (b) **2**, (c) **3** and (d) **4**. The measurements were performed under a nitrogen atmosphere, with a heating rate of 10 °C/min.

5. DSC Analysis

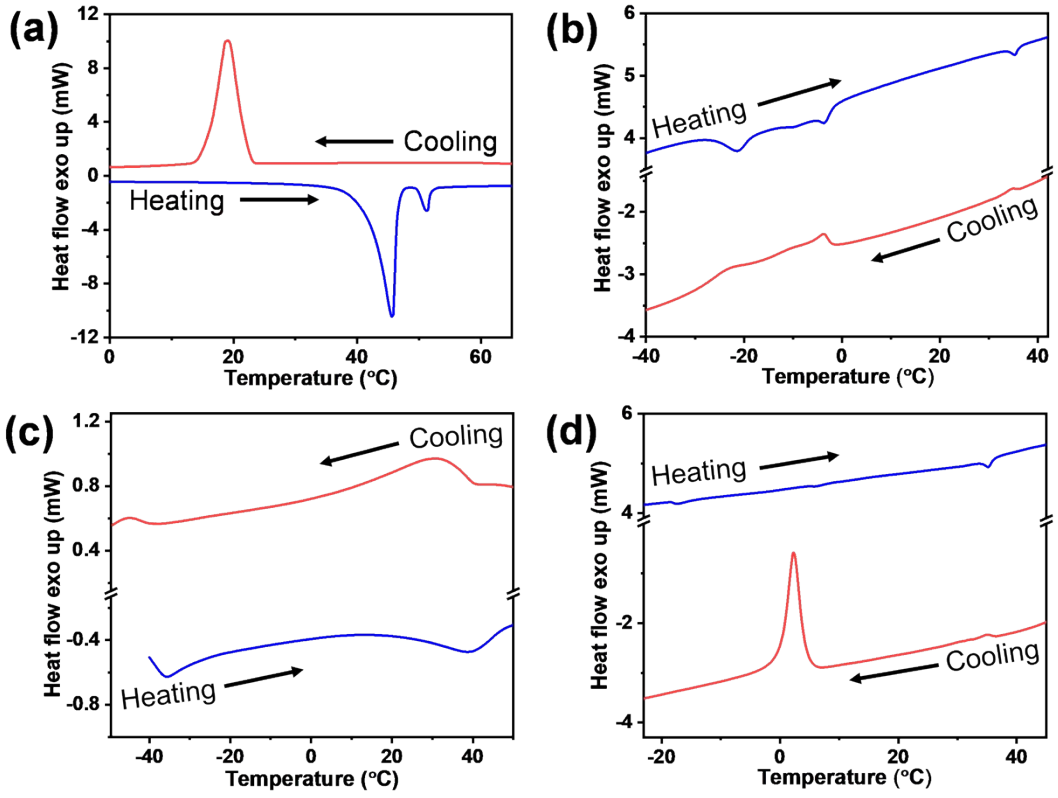

Fig. S11 DSC thermograms of compound (a) **1**, (b) **2**, (c) **3** and (d) **4** on second heating (blue curve) and first cooling (red curve) cycles at the rate of 5 °C/min.

Table S1. Thermal behavior of the synthesized compounds **1-4** [a, b]

Compound	Heating Scan	Cooling Scan[c]
1	Cr 45.58 (55.10) N 51.17 (4.20) I	I 34.5[d] N 19.09 (62.86) Cr
2	Cr_1 -21.07 (9.05) Cr_2 -3.21 (3.42) N* 35.69 (1.81) I	I 34.51 (2.67) N* -4.0 (5.57) Cr_2 -23.7 (3.64) Cr_1
3	Cr -35.72 (3.05) N_D 39.08 (5.84) I	I 30.71 (8.01) N_D -45.07 (0.75) Cr
4	Cr_1 -17.38 (1.32) Cr_2 5.57 (0.72) N_D 35.42 (1.22) I	I 35.04 (2.11) N_D 2.30 (60.15) Cr

[a] Phase transition temperatures (peak) in °C and transition enthalpies in kJ mol^{-1} (in parentheses).

[b] Phase assignments: Cr = Crystalline, N = nematic, N* = chiral nematic, N_D = discotic nematic, I = isotropic.

[c] All enthalpies are in negative.

[d] as observed from POM.

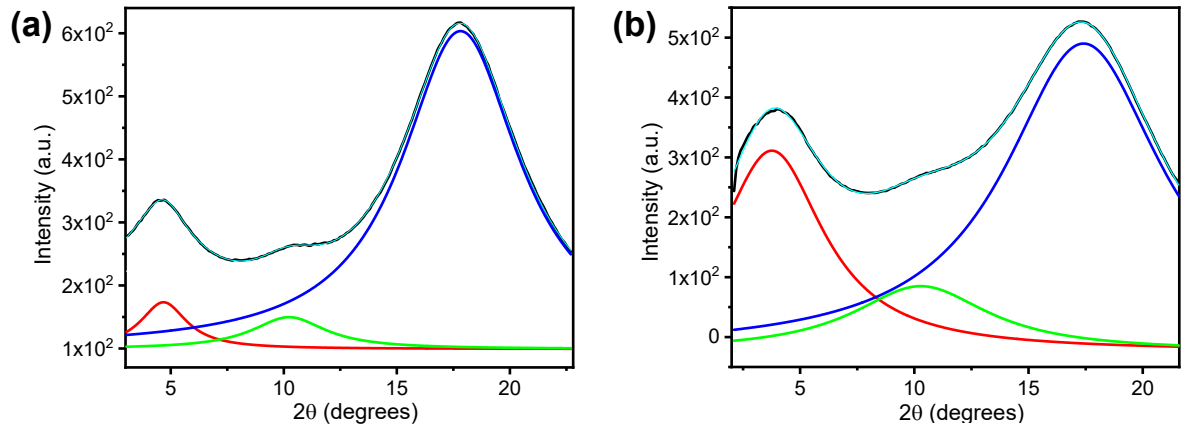

Fig. S12 Deconvoluted XRD patterns of (a) compound **1** and (b) compound **3** in their mesophase.

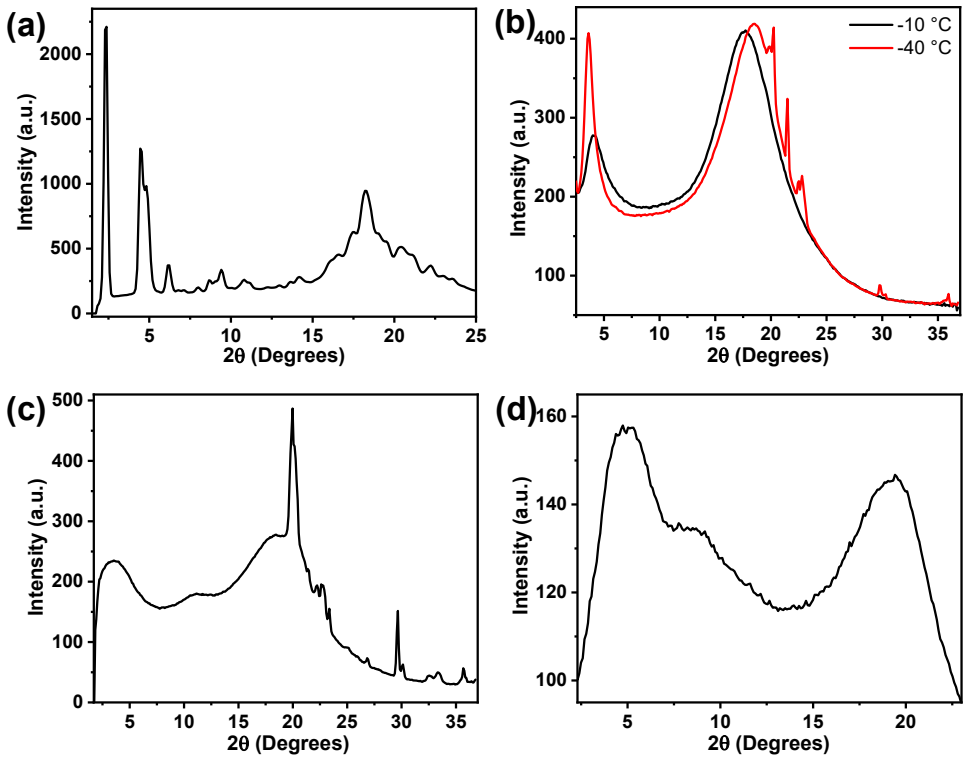

Fig. S13 XRD patterns of (a) compound **1** at 19 °C, (b) compound **2**, (c) compound **3** at -50 °C and (d) compound **4** at 0 °C.

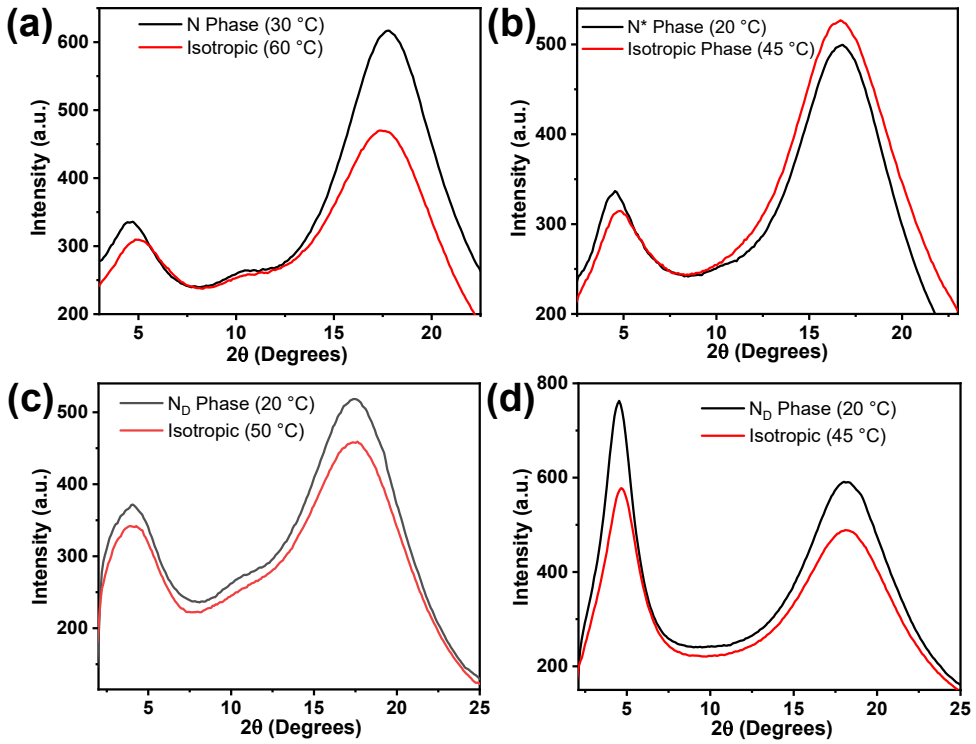

Fig. S14 XRD patterns of (a) compound **1**, (b) compound **2**, (c) compound **3** and (d) compound **4** in their nematic and isotropic phases.

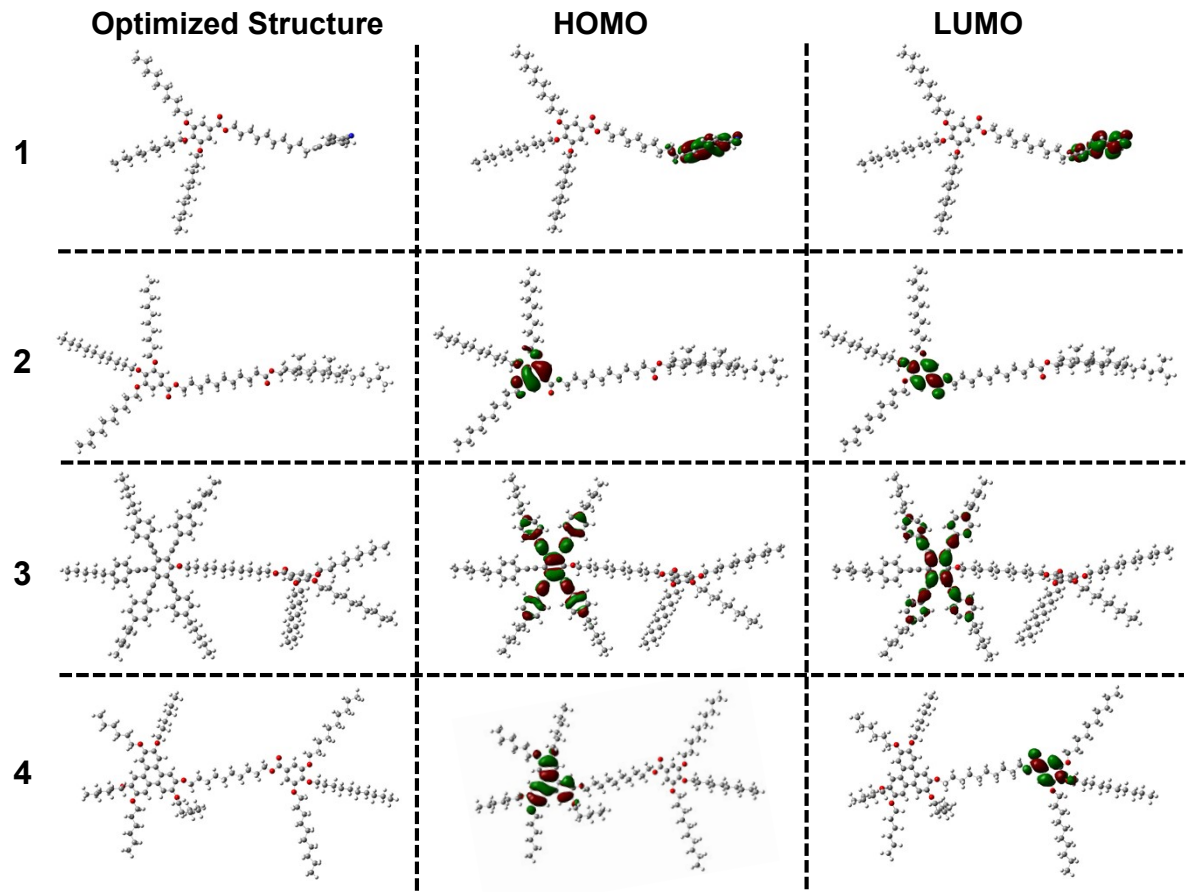

Fig. S15 Optimized geometry and electronic distribution of frontier molecular orbitals (HOMO and LUMO) of compound **1** - **4**.

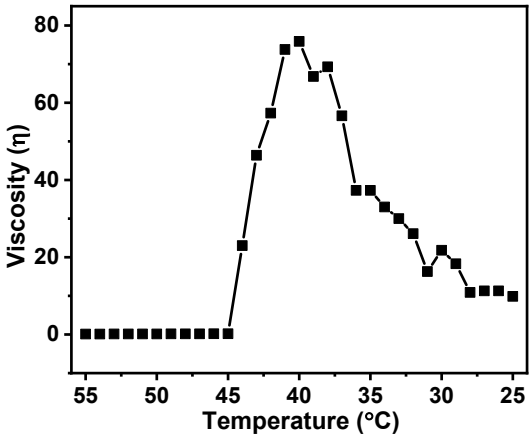

Fig. S16 Temperature dependent viscosity curve for compound **1**. The compound exhibited shear induced crystallization below 45 °C.

References:

1. M. Gupta, Y. Suzuki, T. Sakamoto, M. Yoshio, S. Torii, H. Katayama, T. Kato, *ACS Macro Lett*. **2019**, *8*, 1303-1308.

2. M. Gupta, N. Agarwal, A. Arora, S. Kumar, B. Kumar, G. Sheet and S. K. Pal, *RSC Adv.* **2014**, *4*, 41371-41377.

3. M. Gupta and S. K. Pal, *Liq. Cryst.* **2015**, *42*, 1250-1256.

4. M. Gupta, S. P. Gupta, S. S. Mohapatra, S. Dhara and S. K. Pal, *Chem. Eur. J.* **2017**, *23*, 10626-10631.

5. M. Gupta and S. K. Pal, *Langmuir* **2016**, *32*, 1120–1126.